

# Importance of ZnO nanorods prepared from hydrothermal method for various dyes degradation

N. SRIHARAN<sup>a</sup>, N. MUTHUKUMARASAMY<sup>b</sup>, M. THAMBIDURAI<sup>c</sup>, T. S. SENTHIL<sup>a\*</sup>

<sup>a</sup>Department of Physics, Erode Sengunthar Engineering College, Thudupathi, Erode-638476

<sup>b</sup>Department of Physics, Coimbatore Institute of Technology, Coimbatore-641 014

<sup>c</sup>Luminous Center of Excellence for Semiconductor Lighting and Displays, School of Electrical and Electronic Engineering, Nanyang Technological University, Singapore

Vertically-aligned ZnO nanorods have been prepared by dip coating and hydrothermal method. The crystallinity and morphology of the prepared ZnO nanorods have been studied by using XRD, FE-SEM and UV-Visible spectroscopy. Anionic (Methyl Orange) and cationic (Methylene Blue) dyes were degraded, either individually or in mixtures, by using UV-irradiated ZnO nanorods. High photocatalytic activity results suggest that ZnO nanorod/UV photocatalyst may be envisaged as a method for treatment of dilute colored waste waters not only for degradation, but also for detoxification, especially for the textile industries in semi-arid countries.

(Received April 17, 2017; accepted October 10, 2017)

**Keywords:** Hydrothermal, ZnO nanorods, Anionic and cationic dye, Photocatalytic activity

## 1. Introduction

In recent years, increased industrialization is posing a threat to human health in the form of environmental pollution. The development of environmental remediation of organic pollutants by photocatalytic degradation using wide band gap semiconductor shows great potential with low-cost, environmentally friendly and sustainable water treatment technology. The ability of semiconductor photocatalysts to remove persistent organic compounds and microorganisms in the water has been widely demonstrated [1]. The photocatalytic activity of metal-oxide nanostructures depends on structure, morphology, surface area and surface defects. One-dimensional nanostructures such as nanorods, nanowires and nanotubes are ideal candidates for the application in photocatalysis since they offer a larger surface-to-volume ratio than nanoparticles [2].

The wide direct band gap (~3.37 eV) and large exciton binding energy (~60 meV) of ZnO makes it a promising photocatalyst with low cost and environmental friendliness [3]. When ZnO is irradiated with ultraviolet (UV) light, it can mineralize the water pollutants into non-toxic compounds, such as CO<sub>2</sub> and water [4]. The photocatalytic activity of nanomaterials depends on their size and shape. In particular, smaller nanomaterials are more active compared to their larger counterparts, it is due to the higher surface area exposed to the polluted water [5]. The synthesis of ZnO nanostructures is therefore currently attracting intense interest worldwide. Thus, a great deal of effort has been devoted to synthesize ZnO nanostructures, including nanowires, nanobelts, nanorods and nanohelices [6-8]. ZnO has also been identified as a promising functional material extensively in field emission, short-wavelength optoelectronics, electro-acoustic transducers, gas sensors, transparent conducting

coating materials, piezoelectric devices and photocatalysis [9-11].

Most of the solution routes used for the synthesis of ZnO nanorods need a substrate support, e.g., silicon, glass wafer, Zn sheet and ZnO thin films or nanoparticles as a seed layer [12-14]. ZnO nanorods of various sizes and morphology have been prepared by different methods such as solution growth, conventional sputtering technique, chemical vapor deposition, thermal evaporation, and hydrothermal process [15-19]. Among the various solution routes, sol-gel hydrothermal method is a very attractive and popular method because it can be used to prepare on large area, handy in nature, synthesis is carried out at room temperature and it is easy to control the parameters.

The aim of the present study is threefold: first, to narrow the band gap of ZnO nanorods using different bath temperatures, second, to study their effect on photocatalytic activity in visible light, and third, to ascertain, the versatility of the synthesized ZnO nanorods for the photocatalytic degradation of anionic and cationic dyes and to investigate the active species involved the degradation reaction. Such an approach will no doubt give an objective view on the new materials and their abilities in the light of their possible applications. This should give an insight on the characteristics of an "ideal" photocatalytic material in terms of its structural property and consequently on the conditions of synthesis.

## 2. Experimental

### 2.1. Chemicals

All chemicals used were A.R grade, procured from Alfa Aesar and used without further purification. Double distilled water was used as a medium for the synthesis as well as to prepare the dye solution. Methylene blue

( $C_{16}H_{18}N_3SCl$ ; molecular weight  $373.90 \text{ g}\cdot\text{mol}^{-1}$ ; absorption wavelength  $664.00 \text{ nm}$ ) and methyl orange ( $C_{14}H_{14}N_3NaO_3S$ ; molecular weight  $327.33 \text{ g}\cdot\text{mol}^{-1}$ ; absorption wavelength  $464.50 \text{ nm}$ ) were also purchased from Alfa Aesar. Their molecular structures are shown in Fig. 1 (a & b). A stock solution of dyes was prepared by dissolving 1 g of dye in deionized water using a 1 L volumetric flask. 20 mg/L of dye solutions were prepared by diluting the stock solutions.

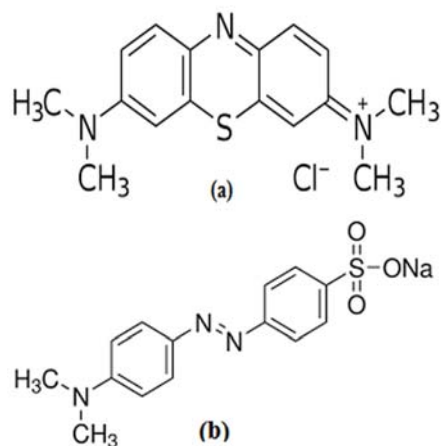


Fig. 1. Chemical structure of dyes: (a) methylene blue; (b) methyl orange

## 2.2. Preparation of ZnO seed layer

To synthesize ZnO nanorods, a two-step chemical method has been used. In the first step, ZnO seed layer has been prepared using sol-gel dip coating method. For the preparation of the ZnO seed layer, 0.2 M zinc acetate dihydrate ( $Zn(CH_3COO)_2\cdot 2H_2O$ ) was dissolved in a mixture of 10 ml ethanol and 0.2 M monoethanolamine ( $NH_2CH_2CH_2OH$ ). The sol-gel dip coating method has been used to prepare ZnO thin film using the prepared solution onto silica glass substrates. The prepared thin films were heated at  $450 \text{ }^\circ\text{C}$  for 1 h and these films form the ZnO seed layer.

## 2.3. Preparation of ZnO nanorods

To prepare ZnO nanorods, an aqueous precursor solution was prepared by dissolving 0.1 M zinc nitrate hexa hydrate ( $Zn(NO_3)_2\cdot 6H_2O$ ) and 1 M hexamethylenetetramine ( $(CH_2)_6N_4$ ) concentration in deionized water which is the best growth layer concentration reported in our work [20] and stirred continuously for 2 h. Then, the seed layer was vertically dipped in the aqueous solution, and it was maintained at a particular bath temperature for 4 h. The ZnO nanorods have been prepared at four different bath temperatures  $80 \text{ }^\circ\text{C}$ ,  $90 \text{ }^\circ\text{C}$ ,  $100 \text{ }^\circ\text{C}$  and  $110 \text{ }^\circ\text{C}$  respectively. At the end of the growth period, the substrates were removed from the solution and were thoroughly washed with deionized water to remove the residual salt from the surface of the film. After this, the prepared films were annealed at  $450 \text{ }^\circ\text{C}$  for 1 h, and this resulted in the formation of ZnO nanorods.

## 2.4. Characterization Techniques

Morphology and sizes of the product were determined by field emission scanning electron microscope (SIGMA HV – Carl Zeiss with Bruker Quantax 200 – Z10 EDS Detector). XRD patterns were recorded using a mini desktop diffractometer X'PERT PRO MPD X-ray diffractometer operated at an accelerating potential of 40 kV and 30 mA filament current with  $CuK\alpha$  radiation of wavelength  $1.5406 \text{ \AA}$  with a scanning rate of 3 per minute (from  $2\theta = 10 \text{ }^\circ\text{C}$  to  $80 \text{ }^\circ\text{C}$ ). Optical absorption spectra were recorded using a UV – VIS double beam spectrometer (SYSTRONICS: AU-2707) in the range of 190–900 nm.

## 2.5. Photocatalytic activities of ZnO nanorods

A specially designed photocatalytic reactor system made of wooden chamber was used for photodegradation experiments. A UV lamp (Philips TUV-08) of 15 W having wavelength  $365 \text{ nm}$  was kept inside the wooden chamber. The hydrothermally grown ZnO nanorods were used as catalyst. The catalyst silica glass substrates with ZnO was kept immersed in the MB solution, the solution was stirred for 10 min, and then kept in the dark for an hour to achieve adsorption equilibrium. When affixed onto the support, ZnO nanorods offer higher surface to volume ratio compared to nano particulate films, allowing higher adsorption of the target molecules [21]. The sample was then transferred into the photoreactor for UV exposure and the lamp was turned on and approximately 5 ml mixture of catalyst and MB or MO solution. The dye solutions with the ZnO film was exposed to light for 5 hours at room temperature. The concentration of MB and MO in the solutions was ascertained by referring to the absorption concentration standard curve which was obtained by measuring the optical absorption of MB and MO at  $665 \text{ nm}$ ,  $464 \text{ nm}$  is using UV-Vis spectrometer.

## 3. Result and discussion

### 3.1. Surface morphology and growth mechanism

Fig. 3 (a–d) FESEM image shows the surface morphology of the ZnO nanorods thin films prepared at different bath temperatures. The images clearly show that the morphology and size of the nanorods are highly dependent on bath temperatures. When the bath temperature is less ( $80 \text{ }^\circ\text{C}$ ), less dense nanorods are formed on the film surface and also it has more spaces between the rods. When the bath temperature is increased to  $90 \text{ }^\circ\text{C}$ , almost nanorods appear on the surface. When the bath temperature is increased to  $100 \text{ }^\circ\text{C}$ , the film surface appears to have nanorods arranged in the form of flowers (Fig. 3c). The reason for the formation of flower like structures at higher bath temperatures may be the initially formed ZnO nanorod nuclei acts as building blocks for the formation of final structures like flowers. With increasing bath temperature, the rate of uniform reaction decreases

because of the quick evaporation of the reactants at higher temperatures and thereby resulting anisotropic growth [22].

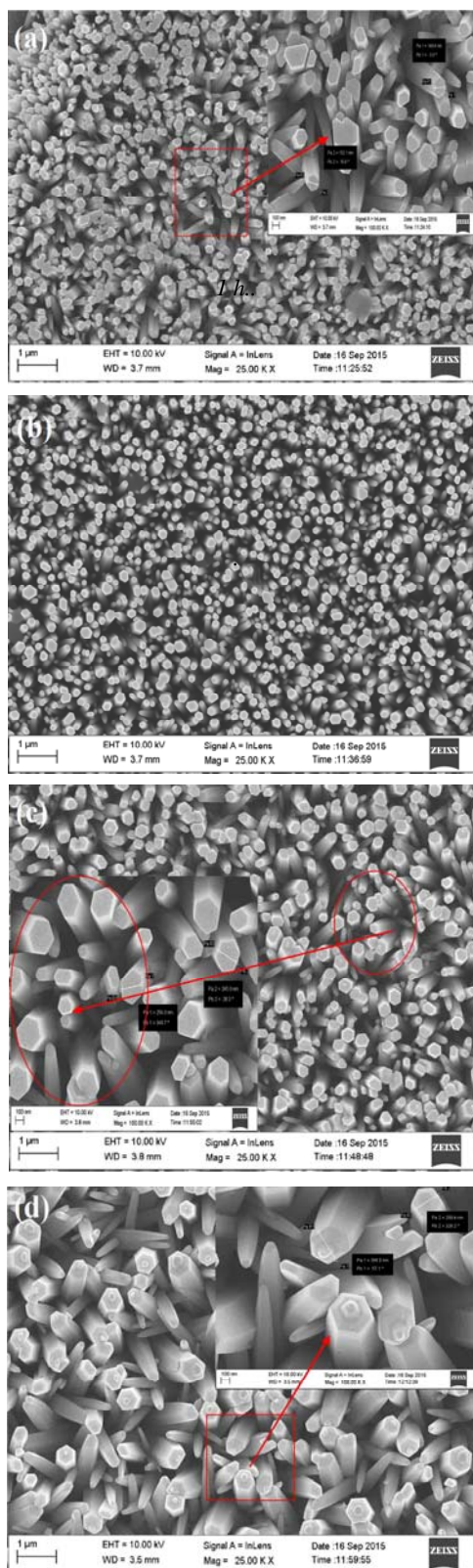


Fig. 1. FESEM image of ZnO nanorods prepared at (a) 80 °C, (b) 90 °C, (c) 100 °C and (d) 110 °C bath temperatures and annealed at 450 °C for 1h.

This result indicates that the bath temperature is also very important for the formation of the ZnO nanorod arrays. Inset of Fig. 3 (d) is higher magnification images of a particular area, it indicates that the ZnO nanorods are of hexagonal shape with the hexagonal pyramid tip. The effective surface area available for photo catalytic dye adsorption is a function of thickness, length and density of the nanorods covering the substrate [23].

### 3.2. X-ray diffraction analysis

X-ray diffraction pattern has been used to investigate the phase of the prepared ZnO nanorods. Fig. 2 shows the X-ray diffraction pattern of the ZnO nanorods prepared at 80 °C, 90 °C, 100 °C and 110 °C bath temperatures. All the diffraction peaks in the diffraction pattern correspond to the hexagonal structure of ZnO. The diffraction peaks at  $2\theta$  (degrees) of 31.7°, 34.5°, 36.3°, 47.7°, 62.9° and 72.5° are respectively, indexed to (100), (002), (101), (102), (103) and (004) planes of ZnO. In all the XRD patterns the peak present at 34.5° is very strong and it shows that the ZnO nanorods are of high c-axis orientation [24]. The lattice parameters have been calculated and are found to be  $a = 3.256 \text{ \AA}$  and  $c = 5.215 \text{ \AA}$  and are in good agreement with the reported standard values (JCPDS No. 36-1451). Within the X-ray diffraction detection limit, there are no other peaks related to impurities, which further confirms that the prepared films are pure ZnO nanorods. The value of the full width at half maxima of these peaks suggests that the grain size is in the nanometer scale. The average crystallite size, micro-strain ( $\epsilon$ ) and dislocation density have been calculated by using the standard formulae [25].

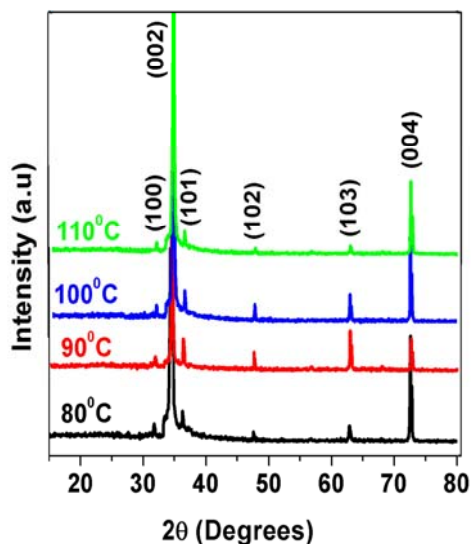


Fig. 2. X-ray diffraction pattern of ZnO nanorods prepared at different bath temperatures and annealed at 450 °C for 1 h

The calculated values of average crystallite size ( $D$ ) micro-strain ( $\epsilon$ ) and dislocation density of the ZnO nanorods thin films prepared at various bath temperatures 80 °C, 90 °C, 100 °C and 110 °C are given in Table 1.

Table 1. Average crystallite size, micro-strain and dislocation density of the synthesized ZnO nanorods thin films prepared at different bath temperatures

ZnO NR'S bath temp.	2θ (Deg.)	D (nm)	Micro-strain, ε	Dislocation density ( $\times 10^{+14}$ Lines/m <sup>2</sup> )
80 °C	34.45	44.84	0.0006	3.145
90 °C	34.47	48.26	0.0008	5.592
100 °C	34.44	54.14	0.0006	3.145
110 °C	34.43	53.13	0.0007	3.144

### 3.3. UV-Visible absorption spectra

Optical absorption in the UV region and corresponding photo efficiency influences the use of ZnO nanorods for photo catalytic activities. Fig. 4 shows the UV-Vis absorption spectra at 370-460 nm for all the ZnO nanorods thin films prepared at different bath temperatures, which is a characteristic band for the wurtzite hexagonal phase of pure ZnO. All the samples show sharp absorption in UV region and high transparency in the visible region. Absorption edge red-shift attributed onto the x-axis and the band gap energy of the samples has been calculated using the formula  $E_g = hc / \lambda$ , where  $h$  and  $c$  are the Planck's constant and the velocity of light respectively, and its values are 3.73, 3.09, 3.02 and 2.95 eV for ZnO nanorod thin films prepared at 80 °C, 90 °C, 100 °C and 110 °C bath temperatures, respectively.

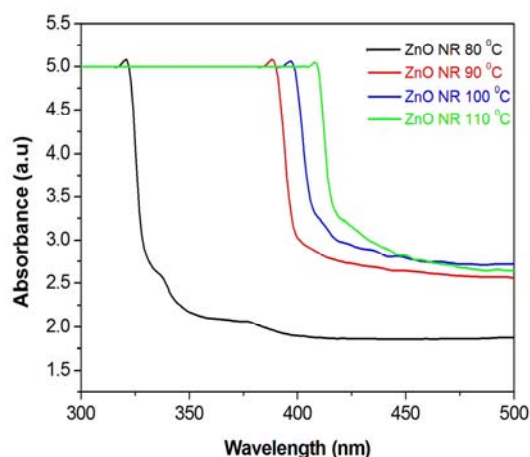


Fig. 4. UV-Visible spectra of the ZnO nanorods Prepared at different bath temperature

It is observed that the band gap decreases with increases in bath temperatures or the absorption edge is shifted toward longer wavelength. This may be due to the formation of difference in morphology and development in crystallinity on annealing. At higher bath temperatures using the hydrothermal method also show an increase in nanorod diameter with different morphology like flowers and pyramid tips on the surface of ZnO nanorod thin films, this causes the decreases of the bandgap. Considering the

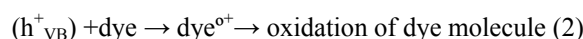
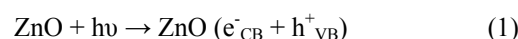
results, it is clearly indicated that as bath temperature increases, the band gap decreases and this difference are due to the change in size, shape of the particles and crystallinity.

### 3.4. Photocatalytic degradation

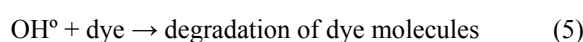
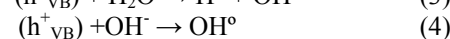
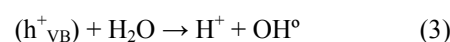
Dyes have different characteristics and affinities. Cationic dyes, such as methylene blue, have more affinity for adsorption and can thus easily be removed by adsorption. Anionic dyes; in which methyl orange dye are very harmful and can cause cancer, have less affinity to adsorption and thus cannot be easily removed [26]. Literature available for synthesis and activity testing of various structured ZnO is abundant, but it deals mostly with dyes as degradation substrates, such as methylene blue (MB) [27], methyl orange (MO) [28], etc., in mg/L scale, with degradation rates ranging from 40% to 98%. The purpose of this study is to assess the capability of photocatalytic degradation of cationic and anionic dyes. The behavior of degradation and adsorption are assessed by the degradation reaction rate. The photocatalytic experiments were carried on the catalyst sample with definite dye concentration (10 ppm). The concentration of the MB and MO dye is estimated using the linear part of the absorbance spectra. The rate of degradation was recorded with respect to the change in intensity of the absorption peak in the visible region.

#### 3.4.1. Impact of UV irradiation and ZnO nanorods thin films photocatalyst

The power of the semiconductor material to act as a sensitizer and to enhance the photodegradation of the dye is based on their electronic structure with the filled valence band and empty conduction band [29]. The semiconductor photoexcitation instigated the photocatalysed degradation of dye in solution and it leaves the catalyst surface with a strong oxidation potential of an electron-hole pair ( $h^+_{VB}$ ) equation (1), when photo catalyst is irradiated with energy higher than that of band gap energy ( $E_g$ ), which allows the oxidation of the dye molecule in a direct manner to the reactive intermediates equation (2).



The hydroxyl radical ( $\text{OH}^\circ$ ), the exceptionally strong and non-selective oxidant which is formed either by decomposition of the water equation (3) or by reaction of the hole along with hydroxyl ion ( $\text{OH}^-$ ). Equation (4) is also responsible for degradation and decolourisation of dye molecule. It leads to the incomplete or complete mineralization of many organic molecules [30].



In this work we have used glass slides as a support for ZnO nanorod photo catalysts. When affixed onto the support, ZnO nanorods offer higher surface to volume ratio compared to nanoparticles, allowing higher adsorption of the target molecules [31]. These high quality ZnO nanorods can be applied as a catalyst for removal of reactive dyes in the industry effluents.

Fig. 5 and 6 shows the typical time dependent UV–Vis absorbance spectrum of MB and methyl orange dye degradation using ZnO nanorods. The prominent peak is observed at  $\lambda_{\text{max}}$  of 664 nm (for MB) and 464 nm (for MO) and it is gradually decreasing with an increase of irradiation time from 1 h to 5 h. The percentage of

degradation (%D) was calculated using the following equation.

$$\text{Percentage of degradation (\%D)} = (A_0 - A_t / A_0) * 100 \quad (6)$$

Where  $A_0$  = absorbance at  $t = 0$  minute

$A_t$  = absorbance at  $t$  minute

For the degradation experiments, fixed amount (0.5 mol/L) of MB and MO dye was taken in a beaker and ZnO nanorods were suspended inside the beaker. The beaker was subjected to UV light irradiation (15 W Philips bulb TUV-08) kept at a distance of 15 cm for a fixed interval of time.

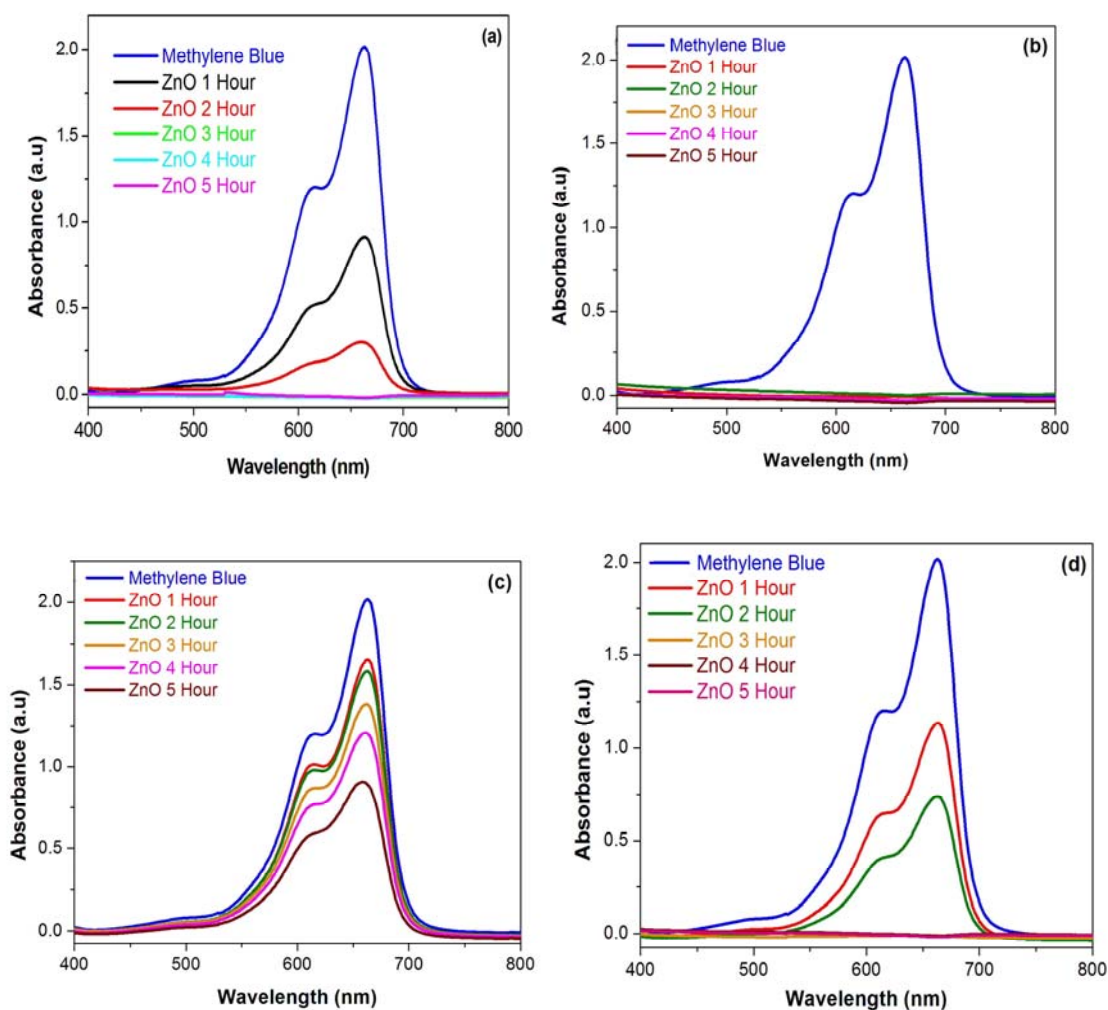


Fig. 5. The time-dependent UV–Vis absorption spectra of degradation of MB using ZnO nanorods thin films prepared at (a) 80 °C (b) 90 °C, (c) 100 °C and (d) 110 °C

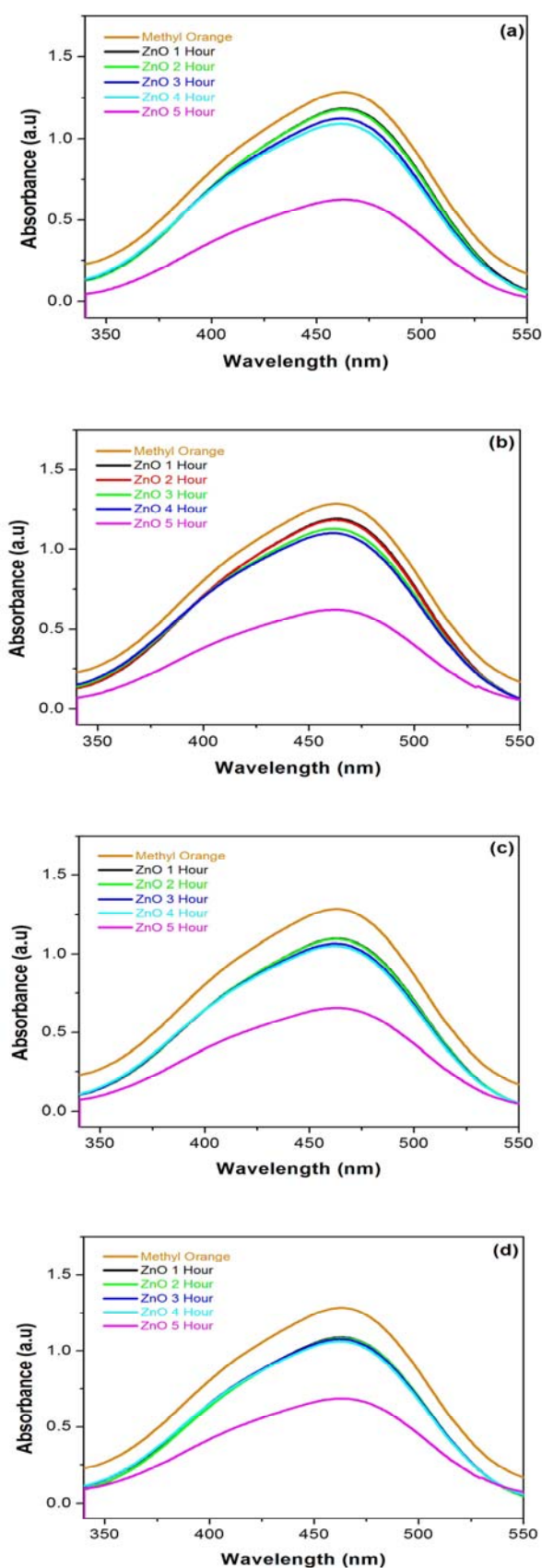


Fig. 6. The time-dependent UV-Vis absorption spectra degradation of MO using ZnO nanorods thin films prepared at (a) 80 °C (b) 90 °C, (c) 100 °C and (d) 110 °C

Fig. 7 and 8 shows the effect of irradiation time of UV on percentage of degradation of MB and MO, respectively, at natural pH. From Fig. 7, it can be clearly seen that the ZnO nanorods prepared at 90 °C shows almost complete degradation even for 1 h UV irradiation, whereas ZnO nanorods prepared at other temperatures shows lower degradation. It clearly shows that even UV irradiation time will not play significant role in MB degradation. This may be due to the enhanced catalyst surface area of ZnO nanorods prepared at 90 °C compared with other bath temperatures. Compared with all bath temperatures ZnO nanorods prepared in 100 °C shows lower photocatalytic degradation it may due to the formation of flower like structures or irregular formation of ZnO nanorods. It may due to the anisotropic growth of ZnO nanorods at higher temperatures. Fig. 8 shows the photocatalytic degradation of MO, the maximum absorption of MO was found to increase with increase of UV irradiation time. The figure clearly shows that even 5 h UV irradiation gives only 50% degradation of MO.

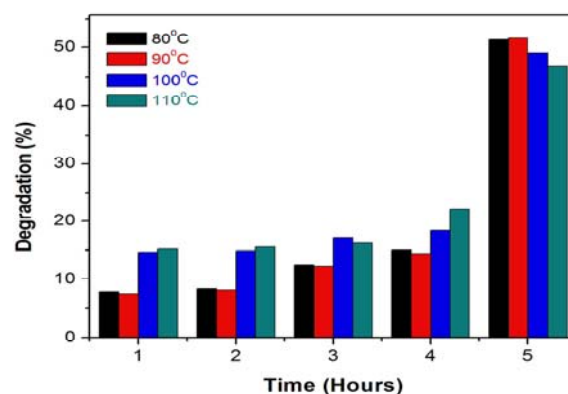


Fig. 7. Effect of irradiation time of MB degradation using ZnO nanorods prepared at different bath temperatures

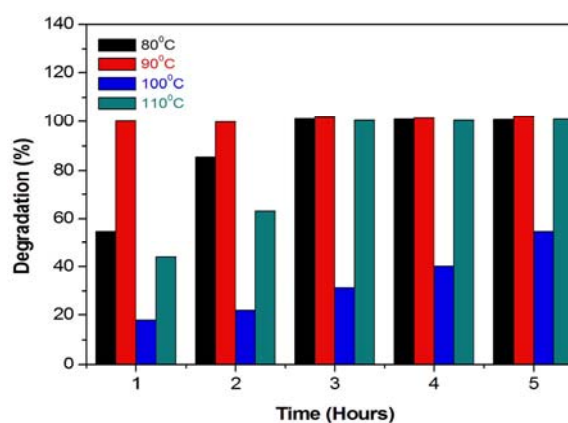


Fig. 8. Effect of irradiation time of MO degradation using ZnO nanorods prepared at different bath temperatures

In particular, the degradation of MB was rapidly achieved to 98% within 1 h of UV irradiation. It was observed that for effective degradation of MB and MO dye solution, both ZnO nanorods photocatalyst and UV light are required. As a result, ZnO nanorods prepared at a bath

temperature of 90 °C display better photocatalytic properties. MB (cationic dye) shows the better degradation compared with MO (anionic dye). Therefore, it can be concluded that the enhancement of photocatalysis depends on the bath temperature of ZnO nanorods, light irradiation time and surface morphology of the ZnO nanorods.

#### 4. Conclusion

ZnO nanorods with different surface morphologies like, flower, bundle and hexagonal shape with pyramid tip were successfully prepared by simple sol-gel dip coating method. FESEM images show that the bath temperature plays an important role in the formation of different nanostructures. XRD analysis shows that the ZnO nanorods exhibit hexagonal wurtzite phase. The photocatalytic degradation of ZnO nanorods was carried out on MB and MO dye by varying irradiation time of photocatalyst. The percentage of photocatalytic degradation results shows that ZnO nanorods prepared at 90 °C bath temperature exhibits best photocatalytic degradation of MB and MO dyes. Therefore, ZnO nanorods may be considered as effective catalyst and it can be used for industrial effluent water treatment process and better recyclability applications.

#### Acknowledgement

We would like to thank the Science and Engineering Research Board (SERB) Sanction Order No and date: SB/FTP/PS-114/2012 Dated 17.09.2013, Department of Science and Technology, New Delhi 110 016 for the financial support.

#### References

- [1] M. N. Chong, B. Jin, C. W. K. Chow, C. Saint, *Water Res.* **44**, 2997 (2010).
- [2] S. Baruah, R. F. Raque, J. Dutta, *NANO: Brief Reports and Reviews* **3**, 8 (2008).
- [3] J. L. Yang, S. J. An, W. I. Park, G.-C. Yi, W. Choi *Adv Mater.* **16**(18), 1661 (2004).
- [4] I. Udom, M. K. Ram, E. H. Stefanakos, A. F. Hepp, D. Y. Goswami, *Mater. Sci. Semicond. Process.* **16**, 2070 (2013).
- [5] S. W. Bian, I. A. Mudunkotuwa, T. Rupasinghe, V. H. Grassian, *Langmuir* **27**, 6059 (2011).
- [6] J. J. Wu, S. C. Liu, *Adv. Mater.* **14**, 215 (2002).
- [7] Z. W. Pan, Z. R. Dai, Z. L. Wang, *Science* **291**, 1947 (2001).
- [8] V. Strano, E. Smecca, V. Depauw, C. Trompoukis, A. Alberti, R. Reitano, I. Cupri, I. Gordon, S. Mirabella, *Appl. Phys. Lett.* **106**, 013901 (2015).
- [9] N. Saito, H. Haneda, T. Sekiguchi, N. Ohashi, I. Sakaguchi, K. Koumoto, *Adv. Mater.* **14**, 418 (2002).
- [10] Z. L. Wang, J. H. Song, *Science*, **312**, 242 (2006).
- [11] F. Lu, W. P. Cai, Y. G. Zhang, *Adv. Funct. Mater.* **18**, 1047 (2008).
- [12] S. Cho, S. Kim, J. W. Jang, S. H. Jung, E. Oh, B. R. Lee, K. H. Lee, *J. Phys. Chem. C* **113**, 10452 (2009).
- [13] H. Zhang, D. R. Yang, X. Y. Ma, N. Du, J. B. Wu D. L. Que, *J. Phys. Chem. B* **110**, 827 (2006).
- [14] G. Wang, D. Chen, H. Zhang, J. Z. Zhang, J. H. Li, *J. Phys. Chem. C* **112**, 8850 (2008).
- [15] X. Fang, L. Peng, X. Shang, Z. Zhang *Thin Solid Films* **519**, 6307 (2011).
- [16] W. T. Chiou, W. Y. Wu, J. M. Ting, *Diam. Relat. Mater.* **12**, 1841 (2003).
- [17] S. C. Lyu, Y. Zhang, H. Ruh, H. J. Lee, H. W. Shim, E. K. Suh, C. J. Lee, *Chem. Phys. Lett.* **363**, 134 (2002).
- [18] Y. G. Wang, C. Yuen, S. P. Lau, S. F. Yu, B. K. Tay, *Chem. Phys. Lett.* **377**, 329 (2003).
- [19] M. Thambidurai, N. Muthukumarasamy, D. Velauthapillai, C. Lee *Mater. Lett.* **92**, 104 (2013).
- [20] J. Deenathayalan, M. Saroja, M. Venkatachalam, P. Gowthaman, T. S. Senthil, *Chalcogenide letters* **8**(9), 549 (2011).
- [21] S. Baruah, R. F. Rafique, J. Dutta, *NANO* **3399**, 407 (2008).
- [22] M. K. Gupta, N. Sinha, B. K. Singh, N. Singh, K. Kumar, B. Kumar, *Mater. Lett.* **63**, 1910 (2009).
- [23] S. Baruah, J. Dutta, *J. Cryst. Growth* **311**, 2549 (2009).
- [24] Oleg Lupan, Lee Chowa, Guangyu Chai, Beatriz Roldan, Ahmed Naitabdi, Alfons Schulte, Helge Heinrich, *Mater. Sci. Engg B* **145**, 57 (2007).
- [25] S. Sivaselvan, S. Muthukumar, M. Ashokkumar, *Opt. Mater.* **36**, 797 (2014).
- [26] E. Fosso-Kankeu, H. Mittal, S. B. Mishra, A. K. Mishra, *Jour. Indust. Engg. Chem.* **22**, 171 (2015).
- [27] P. Amornpitoksuk, S. Suwanboon, S. Sangkanu, A. Sukhoom, N. Muensit, *Super. Microstruct.* **51**, 103 (2012).
- [28] S. Ma, R. Li, C. Lv, W. Xu, X. Gou, *J. Hazard. Mater.* **192**, 730 (2011).
- [29] M. Swaminathan, N. Shobana, *Jour. Separat. Purify. Tech.* **56** (2007) 101.
- [30] S. K. Kansal, M. Singh, D. Sud, *J. Hazard. Mater.* **141**, 581 (2007).
- [31] S. Baruah, R. F. Rafique, J. Dutta, *NANO* **3**, 399, (2008).